

# The Histological Features of a Myocardial Biopsy Specimen in a Patient in the Acute Phase of Reversible Catecholamine-induced Cardiomyopathy due to Pheochromocytoma

Miyuki Miura<sup>1</sup>, Hiroaki Kawano<sup>1</sup>, Takeo Yoshida<sup>1</sup>, Yuki Yamagata<sup>1</sup>, Tomoo Nakata<sup>1</sup>,  
Seiji Koga<sup>1</sup>, Satoshi Ikeda<sup>1</sup>, Kan Kageyama<sup>2</sup>, Kuniko Abe<sup>3</sup> and Koji Maemura<sup>1</sup>

---

## Abstract

---

A 63-year-old Japanese woman with an adrenal tumor was transferred to our hospital due to cardiogenic shock. Right and left ventriculography showed severe hypokinesis of the middle segment and the apex in both ventricles, and an endomyocardial biopsy demonstrated a small number of necrotic myocytes and cellular infiltration. She was diagnosed with pheochromocytoma and quickly recovered after treatment with an  $\alpha$ -blocker. The functional disability of both the right and left ventricles with less myocardial damage due to an excessive level of catecholamine seemed to be related to the early recovery the present patient with catecholamine-induced cardiomyopathy due to pheochromocytoma.

**Key words:** catecholamine, cardiomyopathy, acute heart failure, pathology

(Intern Med 56: 665-671, 2017)

(DOI: 10.2169/internalmedicine.56.7454)

---

## Introduction

---

Pheochromocytoma is a rare, catecholamine-producing tumor of the adrenal medulla that is composed of chromaffin cells. Its incidence is approximately 2-8 per million in the general population and 0.2-0.6% in hypertensive patients (1). The classical symptoms of pheochromocytoma include episodic headache, diaphoresis, and palpitations, but the clinical expression of pheochromocytoma is variable and can be confused with many other diseases (2). Pheochromocytoma can also present with cardiovascular complications, including paroxysmal hypertension, hypotension, cardiogenic shock, pulmonary edema, arrhythmia, ischemic heart disease, and cardiomyopathy (3). Hypertension, either sustained or paroxysmal, is the most common feature of pheochromocytoma; it is reported in 80-90% of patients with pheochromocytoma (3). It has been suggested that pheochromocytoma-related cardiomyopathy is caused by the excessive levels of catecholamine that are released from the

tumor (4); the prevalence of catecholamine-induced cardiomyopathy in pheochromocytoma is 10-11% (1, 5).

However, the precise histological features in the acute phase of reversible left ventricular dysfunction in pheochromocytoma patients with catecholamine-induced cardiomyopathy are unknown. We herein present a case of catecholamine-induced cardiomyopathy in a pheochromocytoma patient, in which histological study of an endomyocardial biopsy specimen revealed myocardial necrosis and cellular infiltration with various types of inflammatory cells.

---

## Case Report

---

A 63-year-old woman was emergently admitted to a primary hospital, 2 days prior to being transferred to our hospital, complaining of palpitations, headache, and nausea. She had been treated for hypertension and had experienced episodic palpitations, headaches, and nausea for several years. On admission, treatment with verapamil (120 mg, t.i.d.) was initiated due to hypertension (170/110 mmHg) and sinus

---

<sup>1</sup>Department of Cardiovascular Medicine, Nagasaki University Graduate School of Biomedical Sciences, Japan, <sup>2</sup>Department of Cardiology, Nagasaki Kita Hospital, Japan and <sup>3</sup>Department of Pathology, Nagasaki University Hospital, Japan

Received for publication March 21, 2016; Accepted for publication July 18, 2016

Correspondence to Dr. Hiroaki Kawano, hkawano@nagasaki-u.ac.jp

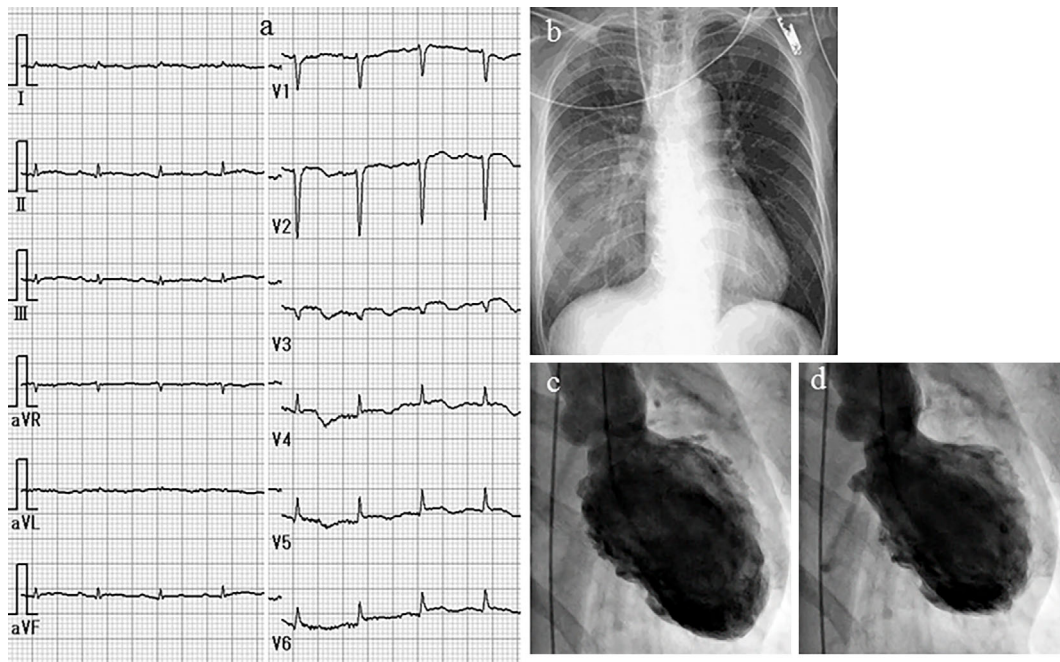


**Figure 1.** The ECG findings. ECG shows sinus rhythm with a heart rate of 120 beats/min, low voltage, poor r wave progression in leads V1-3, a Q wave in lead V3, slight ST segment elevation in leads V2-5, and a negative T wave in leads V2-5 (a). A chest X-ray in the supine position shows right pleural effusion and pulmonary congestion (b). Left ventriculography (LVG) shows severe hypokinesis of the middle segment and apex and the preserved contraction of the basal segment of the left ventricle (c: end-diastolic phase, d: end-systolic phase).

tachycardia (150 beats/min). After medication, her blood pressure was 158/110 mmHg and heart rate was 110 beats/min. A chest X-ray showed cardiomegaly and pulmonary congestion. Electrocardiography (ECG) showed low voltage and negative T waves in leads V2-6. Transthoracic echocardiography (TTE) demonstrated diffuse hypokinesis of the left ventricle, with a left ventricular ejection fraction (LVEF) of 25%. In addition, computed tomography (CT), which had been performed a few years previously, showed an adrenal tumor. She was therefore transferred to our hospital for the treatment and evaluation of heart failure and an adrenal tumor. Upon arrival at our hospital, the patient's blood pressure was 95/73 mmHg, her heart rate was 120 beats/min, her body temperature was 35.7°C, her respiratory rate was 20 breaths/min, and her oxygen saturation on 3 L/min oxygen by nasal cannula was 96%. Third and fourth heart sounds were heard on cardiac auscultation. ECG showed sinus rhythm and a heart rate of 120 beats/min, low voltage, poor r wave progression in leads V1-3, a Q wave in lead V3, slight ST segment elevation in leads V2-5, and negative T waves in leads V2-5 (Fig. 1a). A chest X-ray in the supine position revealed right pleural effusion and pulmonary congestion (Fig. 1b). Echocardiography showed diffuse hypokinesis of the left ventricle, with especially severe hypokinesis from the middle segment to the apex; the LVEF was as low as 20%. The patient's laboratory data included the following findings: white blood cell count, 17,100/mm<sup>3</sup>; blood urea nitrogen, 37 mg/dL; creatinine, 1.14 mg/dL; aspartate aminotransferase, 1,616 IU/L; alanine aminotransferase,

1,801 IU/L; lactate dehydrogenase, 1,337 IU/L; creatine kinase, 1,668 IU/L; creatine kinase MB, 50 ng/mL; high-sensitivity troponin T, 1.25 ng/mL; C-reactive protein, 4.66 mg/dL; N-terminal probrain natriuretic peptide, 23,388 pg/mL. An arterial blood gas analysis revealed hypoxemia (PO<sub>2</sub>, 61.1 mmHg), hypocapnia (PCO<sub>2</sub> 23.5 mmHg) and lactic acidemia (lactate 28.0 mmol/L) with a pH of 7.513. Emergency coronary angiography revealed no coronary artery stenosis. Left ventriculography (LVG) showed severe hypokinesis of the middle segment and apex, and the preserved contraction of the basal segment of the left ventricle (Fig. 1c, d). Right ventriculography (RVG) showed severe hypokinesis, with the exception of the basal segment of the right ventricle (Fig. 2). Intra-aortic balloon pumping (IABP) support was given to maintain the hemodynamic condition. An endomyocardial biopsy of the right ventricle was performed. The biopsied myocardium showed vacuolar degeneration and a contraction band in some myocytes (Fig. 3a). A small number of myocytes were necrotic, and fine fibrosis was also seen (Fig. 3b). Cellular infiltration was observed in the interstitium, and leukocyte infiltration was confirmed by the immunostaining of leukocyte common antigen (CD45) (Fig. 3c). Polymorphonuclear cells (neutrophils) and plasma cells were also seen (Fig. 3d). The following immunohistochemical staining procedures were performed to evaluate the types of infiltrating cells in the myocardium: LeuM1 (CD15) staining for granulocytes including neutrophils, CD3 staining for T-lymphocytes, L26 (CD20) staining for B-lymphocytes, and CD68 staining for macrophages. All types



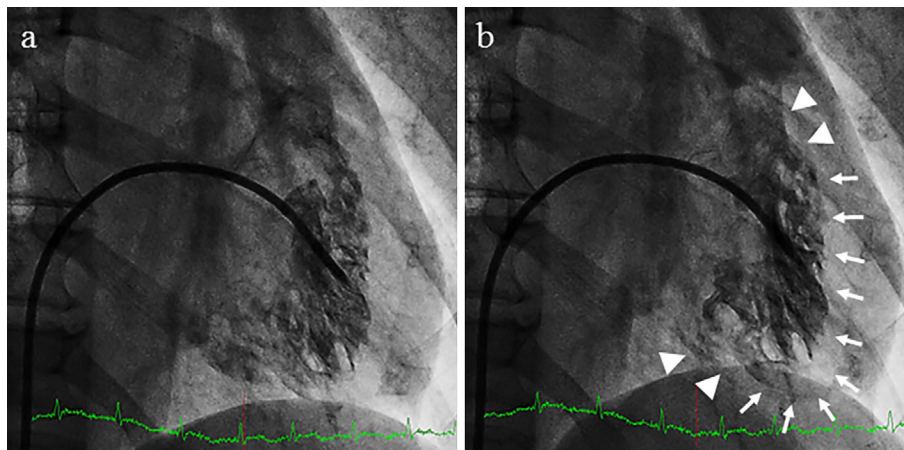


**Figure 2.** Right ventriculography (RVG) shows severe hypokinesia (arrows), with the exception of the basal segment (arrow heads) of the right ventricle (a: end-diastolic phase, b: end-systolic phase).

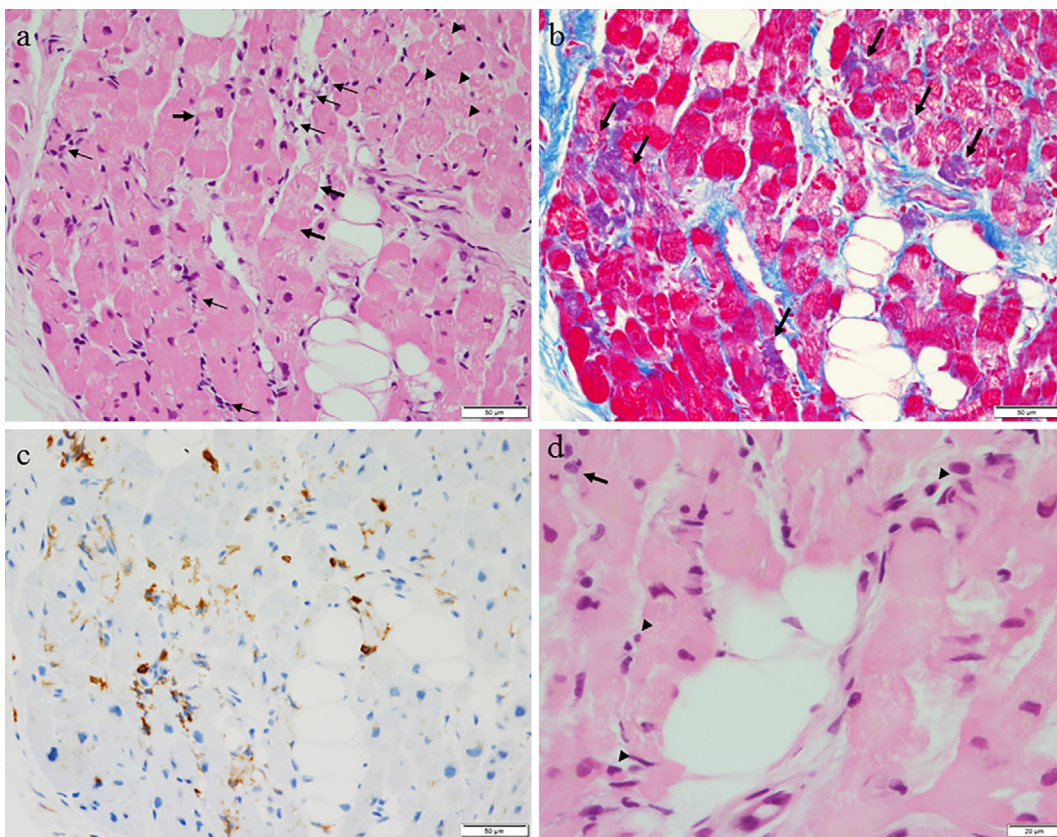


**Figure 3.** The microscopic findings of a biopsy specimen from the endomyocardium of the right ventricle. a: Vacuolar degeneration (arrowheads) and a contraction band (thick arrows) are seen in the myocytes. Cellular infiltration is observed in the interstitium (thin arrows) (Hematoxylin and Eosin staining; scale bar, 50  $\mu$ m). b: Azan staining also demonstrates cellular degeneration (violet-colored myocytes, arrows) and interstitial fibrosis (scale bar, 50  $\mu$ m). c: Leukocyte common antigen (CD45) -positive cells are seen in the interstitium (scale bar, 50  $\mu$ m). d: Polymorphonuclear cells (neutrophils) (arrowheads) and plasma cell (arrows) are also seen (scale 20  $\mu$ m).

of cells were observed among the infiltrating cells. The proportions of the cell types was as follows: T-lymphocytes, 4; macrophages, 2; neutrophils, 2; B-lymphocytes, 1. (Fig. 4). CT showed a right adrenal tumor of 30 mm in diameter (Fig. 5). The strong uptake of  $^{123}\text{I}$ -metaiodobenzylguanidine ( $^{123}\text{I}$ -MIBG) by the adrenal tumor was observed in  $^{123}\text{I}$ -MIBG

scintigraphy on day 8 (Fig. 5b, c). Defects in the uptake of MIBG were also observed from the middle segment to the apex of the left ventricle, while the myocardial uptake of MIBG was maintained in the basal segment of the left ventricle (Fig. 4b, c). A >3-fold elevation of the plasma and urine catecholamine levels was observed on day 1 (Table).

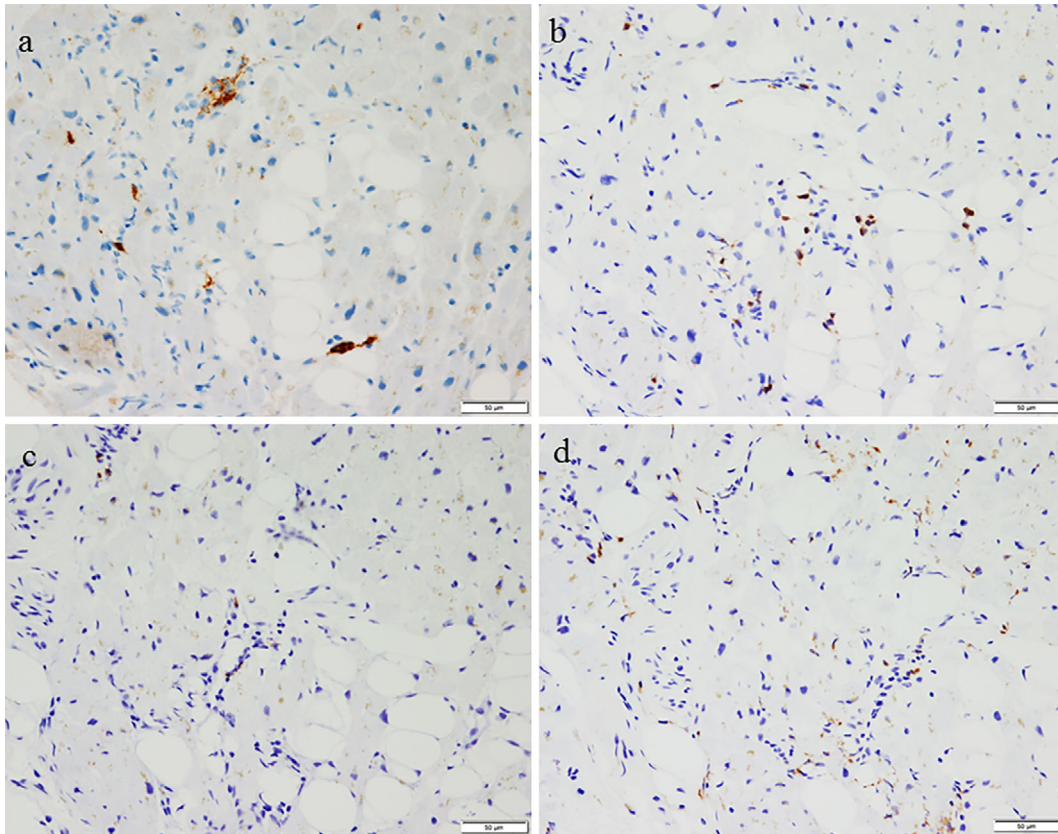


**Figure 4.** Immunostaining of several types of infiltrating cells [a: LeuM1, b: CD3, c: L26 (CD20), d: CD68]. All types of cells are seen among the infiltrating cells, fewer B-cells are observed in comparison to other types of cells (scale bar, 50  $\mu$ m).

**Table.** Plasma and Urine Catecholamine Levels on Day 1.

		Normal range
Plasma		
Epinephrine	4,355 pg/mL	$\leq 100$ pg/mL
Norepinephrine	6,992 pg/mL	100-450 pg/mL
Dopamine	196 pg/mL	$\leq 20$ pg/mL
Urine		
Epinephrine	179.6 $\mu$ g/day	3.4-26.9 $\mu$ g/day
Norepinephrine	240.8 $\mu$ g/day	48.6-168.4 $\mu$ g/day
Dopamine	2,252.3 $\mu$ g/day	365.0-961.0 $\mu$ g/day
Vanillylmandelic acid	10.0 $\mu$ g/mg $\cdot$ Cr	1.2-4.9 $\mu$ g/mg $\cdot$ Cr
Metanephrine	1.77 mg/day	0.04-0.18 mg/day
Normetanephrine	0.83 mg/day	0.10-0.28 mg/day

Tests for viral antibodies (using paired serum samples) against adenovirus, Coxsackie virus (A16, A7, B1, B2, B3, B4, B5, and B6), echovirus (3, 6, 7, 11, and 12), and parainfluenza virus (1, 2, and 3) were all negative. Thus, the patient was diagnosed with catecholamine-induced cardiomyopathy with pheochromocytoma.

Treatment with doxazosin ([an oral  $\alpha$ -blocker] 2 mg), mirlinone ([a PDE3 antagonist] 0.25  $\mu$ g/min/kg), and furosemide (40 mg/day, intravenous) was initiated before coronary angiography, and heparin sodium (10,000 units/day) was started to prevent thromboembolism due to the patient's low cardiac function. On day 2, the patient was started on

gabexate mesilate (1,000 mg/day) because she developed disseminated intravascular coagulation (DIC). At the same time, echocardiography showed hypokinesis of the middle segment to the apex; however, her left ventricular motion had improved, with an LVEF of 43%. On day 4, echocardiography showed normal left ventricular motion and an LVEF of 65%. The patient's DIC resolved with the improvement of her hemodynamic condition, and IABP support was withdrawn. The doses of furosemide, heparin sodium, and gabexate mesilate were tapered. Her doxazosin dose was increased to 4 mg/day on day 5 and was gradually increased to 12 mg/day over 2 weeks. On day 7, her LVEF improved to 78%. Her NT-pro BNP level decreased to 62.53 pg/mL. The patient was discharged on day 19. Four weeks later, she was admitted to the urological department of our hospital, and the adrenal tumor was surgically removed. A histological examination of the tumor with immunohistochemistry confirmed the diagnosis of pheochromocytoma (Fig. 5d, e). The patient's plasma catecholamine levels normalized soon after surgery. Her blood pressure and plasma catecholamine levels remained within the normal range without antihypertensive drug therapy at a 12-month follow-up examination.

## Discussion

The present report demonstrated vacuolar myocyte degen-



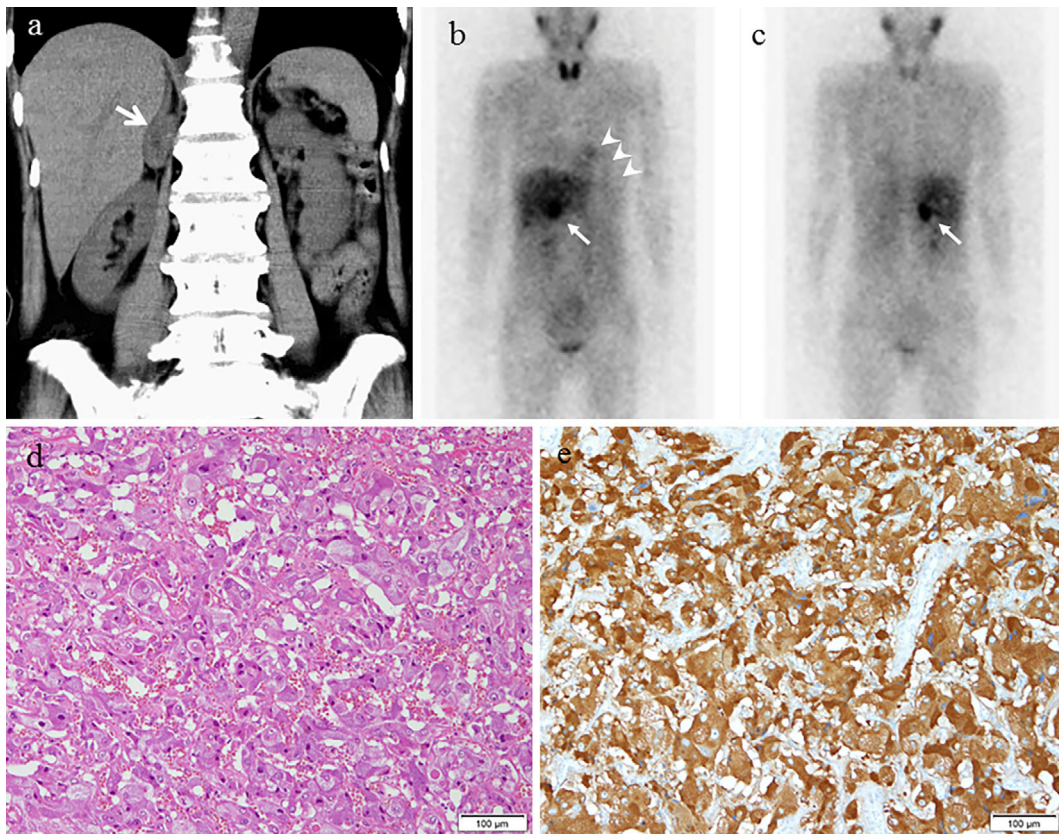


**Figure 5.** CT,  $^{123}\text{I}$ -MIBG scintigraphy, and the histopathology of the adrenal tumor. A 30-mm right adrenal tumor (arrows) is observed on CT (a). The strong uptake of the adrenal tumor is observed on  $^{123}\text{I}$ -MIBG scintigraphy (b: anterior view, c: posterior view) (arrows), uptake of MIBG in the myocardium is low (arrowheads). The histopathological findings are consistent with pheochromocytoma (d: Hematoxylin and Eosin staining, scale bar: 50  $\mu\text{m}$ , e: immunostaining with chromogranin A).

eration, the mild contraction band formation of myocytes, a small number of necrotic myocytes, focal fine interstitial fibrosis, and cellular infiltration in the biopsied myocardium of a patient with catecholamine-induced cardiomyopathy and pheochromocytoma.

Previous autopsy studies and experimental animal studies have demonstrated that catecholamines produce myocardial damage (6), and that the myocardial damage in patients with pheochromocytoma is indistinguishable from that produced in experimental animals by catecholamine infusion (7). According to a catecholamine infusion experiment, the early histological findings include interstitial edema, subendocardial congestion, and hemorrhage (8). Myofibrillar degeneration has been demonstrated immediately after a bolus injection of catecholamine (9). Contraction bands may also occur; however, they are not specific to the catecholamine-induced cardiomyopathy that occurs in patients with pheochromocytoma. Within hours after the injection of catecholamine, infiltration appears with polymorphonuclear cells followed by lymphocytes (6, 9). After 3 days, the number of polymorphonuclear cells decreases, and plasma cells are occasionally found and fine collagen connective tissues appear. The resorption of necrotic myocytes and granulation tissue becomes prominent by the sixth day, which is progressively

replaced by fibrosis, and only scar tissue remains at two weeks (6, 9).

Thus, the histological findings in the present patient indicate that the biopsy was performed at approximately 2-3 days after the initiation of myocardial injury due to an excess level of catecholamine. These findings are compatible with the clinical course. There are only two reports of the endomyocardial biopsy findings in patients who were diagnosed with catecholamine-induced cardiomyopathy and pheochromocytoma; both of whom recovered after treatment (10, 11).

Iio et al. (10) demonstrated neutrophilic infiltration and diffuse contraction-band necrosis in a myocardial biopsy specimen that was taken on admission in a patient with cardiogenic shock due to pheochromocytoma and inverted Takotsubo cardiomyopathy-like wall motion of the LV. In their case, the neutrophilic infiltration that occurred in association with contraction band necrosis might have been related to the acute phase or to the administration of catecholamine, which is used to treat cardiogenic shock in patients with severe catecholamine-induced cardiomyopathy and pheochromocytoma.

On the other hand, Yamanaka et al. (11) showed lymphocytic infiltration, disorganized myocardial tissue, and fine

proliferative collagen fibers in the myocardium in a biopsy specimen that was obtained after the recovery of LV function at 11 days after admission. These results indicate that the histological features of catecholamine-induced cardiomyopathy in patients with pheochromocytoma are affected by the timing of the myocardial biopsy from the onset of myocardial damage, which is caused by the excess level of catecholamine that occurs due to pheochromocytoma.

The types of infiltrating cells are also important for the diagnosis of myocardial disease, especially myocarditis. For example, the presence of eosinophils indicates eosinophilic myocarditis, while the presence of lymphocytes indicates lymphocytic (or viral) myocarditis. The present report also demonstrated that various types of cells, including neutrophils, T-lymphocytes, macrophages, and B-lymphocytes infiltrated around the degenerative or necrotic myocytes. Previous studies indicated that inflammatory cell infiltration occurs in response to myocardial damage in patients with pheochromocytoma (7, 12). The presence of these findings in the present patient seems to be compatible with myocardial damage.

However, there no reports have precisely evaluated the types of infiltrating cells in the myocardium of patients with catecholamine-induced cardiomyopathy and pheochromocytoma.

Takotsubo cardiomyopathy (or stress cardiomyopathy) is another type of catecholamine-induced cardiomyopathy, and endomyocardial biopsies in some Takotsubo cardiomyopathy patients have demonstrated contraction band necrosis and mononuclear cell infiltration, similar to the findings that are observed in patients with pheochromocytoma (13). Nef et al. (14) showed that macrophages and T-lymphocytes were detected in the acute phase and the recovered myocardium in patients with Takotsubo cardiomyopathy. Thus, infiltration by macrophage and T-lymphocytes may be common findings in patients with catecholamine-induced cardiomyopathy.

In fact, in the present case, <sup>123</sup>I-MIBG scintigraphy revealed defects in the uptake of MIBG in the middle segment to the apex of the left ventricle and the maintained myocardial uptake of MIBG in the basal segment of the left ventricle. This finding was compatible with the findings in a previous report on catecholamine-induced cardiomyopathy (15); we also observed Takotsubo cardiomyopathy-like wall motion in the LV.

However, there have been no reports about neutrophilic infiltration in the myocardium in Takotsubo cardiomyopathy patients in whom the pathogenic mechanism was not determined. Thus, there may be some differences in the precise mechanisms of myocardial damage and repair in patients with catecholamine-induced cardiomyopathy due to pheochromocytoma and that in patients with catecholamine-induced cardiomyopathy due to Takotsubo cardiomyopathy.

The present patient had an early recovery from heart failure and cardiogenic shock after the initiation of doxazosin and the treatment of heart failure, which included IABP. The examination of the myocardial biopsy specimen revealed a

small number of necrotic myocytes. This indicates that the patient's heart failure and cardiogenic shock were likely to have been mainly due to a functional disability rather than organic damage (such as myocardial injury via  $\alpha_1$ -adrenergic receptors).

Recent reports have suggested the involvement of right ventricular dysfunction and a catastrophic course in patients with Takotsubo cardiomyopathy (16); the present case was consistent with these observations. Thus, it is likely that the right ventricular dysfunction is mainly due to a functional disability and may be another important factor that was associated with the collapsing hemodynamics that were observed in the present patient.

Several mechanisms may be responsible for the acute and chronic myocardial damage associated with catecholamines. These include a direct toxic effect on the myocardium through changes in autonomic tone, enhanced lipid mobility, calcium overload, free radical production, increased sarcolemmal permeability, and myocardial damage secondary to a sustained increase in the myocardial oxygen demand and/or a decrease in the myocardial oxygen supply due to catecholamine-induced coronary arterial vasoconstriction or platelet aggregation (17). These different mechanisms may induce different histological changes in the myocardium of patients with catecholamine-induced cardiomyopathy, and further studies are needed to elucidate the precise mechanisms underlying this condition and the myocardial damage that occurs.

In conclusion, the functional disability of both the right and left ventricles with less myocardial damage due to an excess level of catecholamine seems to be related to the severe heart failure, cardiogenic shock and early recovery that were observed following treatment, which included the administration of an  $\alpha$ -blocker, in a patient with catecholamine-induced cardiomyopathy.

**The authors state that they have no Conflict of Interest (COI).**

## References

1. Peppachan JM, Raskauskiene D, Sriraman R. Diagnosis and management of pheochromocytoma: a practical guide to clinicians. *Curr Hypertens Rep* **16**: 442, 2014.
2. Galetta F, Franzoni F, Bernini G. Cardiovascular complications in patients with pheochromocytoma: A mini-review. *Biomed Pharmacother* **64**: 505-509, 2010.
3. Prejibisz A, Lenders JW, Eisenhofer G, Januszewicz A. Cardiovascular manifestations of phaeochromocytoma. *J Hypertens* **29**: 2049-2060, 2011.
4. Jindal V, Baker ML, Aryangat A. Pheochromocytoma: presenting with regular cyclic blood pressure and inverted Takotsubo cardiomyopathy. *J Clin Hypertens* **11**: 81-86, 2009.
5. Park JH, Kim KS, Sul JY, et al. Prevalence and patterns of left ventricular dysfunction in patients with pheochromocytoma. *J Cardiovasc Ultrasound* **19**: 76-82, 2011.
6. Jiang JP, Downing SE. Catecholamine cardiomyopathy: review and analysis of pathogenetic mechanisms. *Yale J Biol Med* **63**: 581-591, 1990.

7. Kassim TA, Clarke DD, Mai VQ, Clyde PW, Mohamed Shakir KM. Catecholamine-induced cardiomyopathy. *Endocr Pract* **14**: 1137-1149, 2008.
8. Schenk EA, Moss AJ. Cardiovascular effects of sustained norepinephrine infusions. II. Morphology. *Circ Res* **18**: 605-615, 1966.
9. Haft JI. Cardiovascular injury induced by sympathetic catecholamines. *Prog Cardiovasc Dis* **17**: 73-86, 1974.
10. Iio K, Sakurai S, Kato T. Endomyocardial biopsy in a patient with hemorrhagic pheochromocytoma presenting as inverted Takotsubo cardiomyopathy. *Heart Vessels* **28**: 255-263, 2013.
11. Yamanaka O, Yasumasa F, Nakamura T, et al. "Myocardial stunning"-like phenomenon during a crisis of pheochromocytoma. *Jpn Circ J* **58**: 737-742, 1994.
12. Sardesai SH, Mourant AJ, Sivathandon Y, Farrow R, Gibbons DO. Pheochromocytoma and catecholamine induced cardiomyopathy presenting as heart failure. *Br Heart J* **63**: 234-237, 1990.
13. Bybee KA, Prasad A. Stress-related cardiomyopathy syndromes. *Circulation* **118**: 397-409, 2008.
14. Nef HM, Möllmann H, Kostin S, et al. Tako-Tsubo cardiomyopathy: intraindividual structural analysis in the acute phase and after functional recovery. *Eur Heart J* **28**: 2456-2464, 2007.
15. Suga K, Tsukamoto K, Nishigauchi K. Iodine-123-MIBG imaging in pheochromocytoma with cardiomyopathy and pulmonary edema. *J Nucl Med* **37**: 1361-1364, 1996.
16. Elesber AA, Prasad A, Bybee KA, et al. Transient cardiac apical ballooning syndrome: prevalence and clinical implications of right ventricular involvement. *J Am Coll Cardiol* **47**: 1082-1083, 2006.
17. Lange RA, Hillis LD. Toxins and the hearts. In: Braunwald's Heart Disease. A Textbook of Cardiovascular Medicine. 9th ed. Bonnow RO, Mann DL, Zipes DP, Libby P, Braunwald E, Eds. Elsevier Saunders, Philadelphia, 2012: 1628-1637.

The Internal Medicine is an Open Access article distributed under the Creative Commons Attribution-NonCommercial-NoDerivatives 4.0 International License. To view the details of this license, please visit (<https://creativecommons.org/licenses/by-nc-nd/4.0/>).